

NBS

Technical Note

192

CALCULATIONS OF THE POTENTIAL AND EFFECTIVE DIFFUSION CONSTANT IN A POLYELECTROLYTE SOLUTION

SAM R. CORIELL AND JULIUS L. JACKSON



U. S. DEPARTMENT OF COMMERCE
NATIONAL BUREAU OF STANDARDS

THE NATIONAL BUREAU OF STANDARDS

Functions and Activities

The functions of the National Bureau of Standards are set forth in the Act of Congress, March 3, 1901, as amended by Congress in Public Law 619, 1950. These include the development and maintenance of the national standards of measurement and the provision of means and methods for making measurements consistent with these standards; the determination of physical constants and properties of materials; the development of methods and instruments for testing materials, devices, and structures; advisory services to government agencies on scientific and technical problems; invention and development of devices to serve special needs of the Government; and the development of standard practices, codes, and specifications. The work includes basic and applied research, development, engineering, instrumentation, testing, evaluation, calibration services, and various consultation and information services. Research projects are also performed for other government agencies when the work relates to and supplements the basic program of the Bureau or when the Bureau's unique competence is required. The scope of activities is suggested by the listing of divisions and sections on the inside of the back cover.

Publications

The results of the Bureau's research are published either in the Bureau's own series of publications or in the journals of professional and scientific societies. The Bureau publishes three periodicals available from the Government Printing Office: The Journal of Research, published in four separate sections, presents complete scientific and technical papers; the Technical News Bulletin presents summary and preliminary reports on work in progress; and the Central Radio Propagation Laboratory Ionospheric Predictions provides data for determining the best frequencies to use for radio communications throughout the world. There are also five series of nonperiodical publications: Monographs, Applied Mathematics Series, Handbooks, Miscellaneous Publications, and Technical Notes.

A complete listing of the Bureau's publications can be found in National Bureau of Standards Circular 460, Publications of the National Bureau of Standards, 1901 to June 1947 (\$1.25), and the Supplement to National Bureau of Standards Circular 460, July 1947 to June 1957 (\$1.50), and Miscellaneous Publication 240, July 1957 to June 1960 (includes Titles of Papers Published in Outside Journals 1950 to 1959) (\$2.25); available from the Superintendent of Documents, Government Printing Office, Washington 25, D.C.

NATIONAL BUREAU OF STANDARDS

Technical Note 192

ISSUED JUNE 28, 1963

CALCULATIONS OF THE POTENTIAL AND EFFECTIVE DIFFUSION CONSTANT IN A POLYELECTROLYTE SOLUTION

Sam R. Coriell and Julius L. Jackson

NBS Technical Notes are designed to supplement the Bureau's regular publications program. They provide a means for making available scientific data that are of transient or limited interest. Technical Notes may be listed or referred to in the open literature.

Contents

	Page
1. Introduction -----	1
2. Model and Calculations -----	3
3. Discussion -----	7

CALCULATIONS OF THE POTENTIAL AND EFFECTIVE DIFFUSION CONSTANT IN A POLYELECTROLYTE SOLUTION

Sam R. Coriell and Julius L. Jackson

The results of numerical computations of the electrostatic potential and the effective diffusion constant of counterions in a polyelectrolyte solution are given. The potentials for various polyion charge densities and polyion sizes are presented graphically. The calculated diffusion constants are compared with experimental data on the diffusion of labeled sodium ions in polyacrylic acid-sodium hydroxide solutions.

1. Introduction

The diffusion of ions in a periodic electric field was considered as a model for the diffusion of radioactive counterions in a polyelectrolyte solution by Lifson and Jackson.¹ On the basis of the theory of first transit times, they obtained an explicit expression for the observed or effective diffusion constant D' in terms of the hydrodynamic diffusion constant D and the periodic potential $\Psi(\underline{r})$ for a one dimensional model. Jackson and Coriell (JC)² have given a general theory of the effective diffusion constant of ions in a periodic electric field in any number of dimensions. The calculation of the diffusion ratio D'/D is reduced to the solution of a particular boundary value problem over one periodic unit or cell.

The effective diffusion constant D' was shown to be given by

$$D' = \frac{D \int_V e^{-\Phi} \left(1 + \frac{\partial g}{\partial x} \right) dV}{\int_V e^{-\Phi} dV} \quad (1)$$

Here D is the hydrodynamic diffusion constant and Φ is the reduced potential, $e\Psi/kT$. The integrations are over one unit cell. The function g is a solution of the partial differential equation

$$\nabla^2 g - \nabla g \cdot \nabla \Phi = \frac{\partial \Phi}{\partial x} \quad (2)$$

with boundary conditions (for a cube of side $2l_0$)

¹ S. Lifson and J. L. Jackson, J. Chem. Phys. 36, 2410 (1962).

² J. L. Jackson and S. R. Coriell, J. Chem. Phys. 38, 959 (1963).

$$g(\pm l_0, y, z) = 0$$

$$\frac{\partial g}{\partial y}(x, \pm l_0, z) = 0 \quad (3)$$

$$\frac{\partial g}{\partial z}(x, y, \pm l_0) = 0$$

For the periodic model of a polyelectrolyte solution, the potential $\Psi(\underline{r})$ is assumed to be given by the solution of the Poisson-Boltzmann Equation

$$\nabla^2 \Psi(\underline{r}) = - \frac{4\pi e}{\epsilon} \left\{ -\rho(r) + K \exp \left[-e\Psi(\underline{r})/kT \right] \right\}, \quad (4)$$

with $\nabla\Psi \cdot d\underline{S} = 0$ on the surface. Here e is the absolute value of the electronic charge, k is the Boltzmann constant, T is the absolute temperature, and ϵ is the dielectric constant. $[-e\rho(r)]$ is the charge density of the polyelectrolyte³ and $eK \exp(-e\Psi/kT)$ is the charge density of the mobile ions. The constant K is arbitrary, determining the zero of the potential. In JC, values of the effective diffusion constant were obtained by approximate methods---the electrostatic potential in the polyelectrolyte solution was approximated by adopting the results of calculations by Wall and Berkowitz⁴ for spherical geometry and bounds on the effective diffusion constant were obtained by using variational principles for D' rather than following the straightforward procedure of solving Eq. 2 and inserting the result in Eq. 1.

In this article, we report on the results of numerical computations for the potential in a polyelectrolyte solution and the effective diffusion constant. We present graphs of the potential for various charge densities and polyion sizes along with the corresponding values of D' . The calculated values of the effective diffusion constant are⁵ compared with the experimental results of Huizenga, Grieger, and Wall⁵ for the diffusion of labeled sodium ions in polyacrylic acid-sodium hydroxide solutions. The values of the effective diffusion constant, obtained numerically, in most cases fall within the bounds which were calculated in JC for an approximate potential.

³ For our purposes here, we will regard the polymer charge distribution as a given function of \underline{r} , rather than attempt to write its dependence on the potential, an approach which introduces a greater order of complexity.

⁴ (a) F. T. Wall and J. Berkowitz, J. Chem. Phys. 26, 114 (1956); (b) J. Berkowitz, Ph.D. thesis, University of Illinois, 1955.

⁵ J. R. Huizenga, P.F. Grieger, and F. T. Wall, J. Am. Chem. Soc. 72, 4228 (1950)

2. Model and Calculations

We assume the following model for a polyelectrolyte solution. Each polyion is assigned to an identical cube of volume V , the center of the polyion coinciding with the center of the cube. The center of the cube is taken as the origin of an (x, y, z) coordinate system. The distribution of counterions in each cube is proportional to $\exp(-e\psi/kT)$. Two different models have been employed for the polyion charge density, $-e\rho(\underline{r})$. In the uniform sphere model the polyion charge density ρ_s is uniformly distributed over a sphere of volume v , and is zero outside of the sphere. In the Gaussian model a Gaussian distribution of polyion charge is assumed, i.e., $\rho_s = a \exp(-br^2)$, where a and b are constants which will be specified subsequently. The potential Ψ is given by the Poisson-Boltzmann equation (Eq. 4). Wall and Berkowitz have solved this equation for the uniform sphere model with spherical symmetry, i.e., the boundary conditions are specified on a sphere rather than on a cube.

In terms of the polyion concentration c , and the degree of polymerization s , the volume V per polyion is

$$V = \frac{1000s}{cN} \quad , \quad (5)$$

where V is in cm^3 , c in moles of monomer per liter, and N is Avogadro's number. The charge density ρ on the polyion is related to per cent neutralization p by

$$\int_V \rho dV = \frac{ps}{100} \quad , \quad (6)$$

where the integral is over the volume of one cube. For the uniform sphere model, the above equation becomes

$$Av = A(4/3) \pi r_o^3 = ps/100 \quad , \quad (7)$$

where r_o is the radius of the sphere or polyion and $-eA$ is the polyion charge density in the sphere.

The Poisson-Boltzmann equation, Eq. (4), may be written in a more convenient form by introduction of the reduced potential $\Phi = e\psi/kT$ and dimensionless variables (X, Y, Z) such that $X = x/l_o$, $Y = y/l_o$, and $Z = z/l_o$, where $2l_o$ is the length of the edge of the periodic cube, i.e., $V = 8l_o^3$. Eq. (4) then becomes

$$\nabla^2 \Phi = \frac{4\pi e^2}{\epsilon kT} l_o^2 \left\{ \rho - K \exp(-\Phi) \right\} \quad (8)$$

Since K is arbitrary, we can take it equal to $(\epsilon kT/4\pi e^2 l_o^2)$. A different choice of K simply changes Ψ by a constant amount. For the uniform sphere model, the Poisson-Boltzmann Equation can be written as

$$\nabla^2 \Phi = c_1 S(R) - \exp(-\Phi), \quad (9)$$

where $R = [X^2 + Y^2 + Z^2]^{1/2}$, $S(R)$ is a step function equal to unity for $R \leq r_0/\ell$ and equal to zero for $R > r_0/\ell$, and $c_1 = 4\pi e^2 \ell^2 A/\epsilon kT$. Using Eqs. (5) and (7), c_1 may be written as

$$c_1 = \frac{3e^2 p(s^2 c_N)^{1/3} \ell_o^3}{500 \epsilon kT r_o^3} \quad (10)$$

For $T = 298^\circ K$, and $\epsilon = 78$

$$c_1 = .03645 p(s^2 c)^{1/3} (\ell_o/r_o)^3. \quad (11)$$

The boundary conditions on the Poisson-Boltzmann Equation, Eq. (9), are

$$\begin{aligned} \frac{\partial \Phi}{\partial X}(X = \pm 1) &= 0, & \frac{\partial \Phi}{\partial Y}(Y = \pm 1) &= 0, & \text{and} \\ \frac{\partial \Phi}{\partial Z}(Z = \pm 1) &= 0. \end{aligned} \quad (12)$$

Because of the symmetry of the potential, i.e., $\Phi(X, Y, Z) = \Phi(\pm X, \pm Y, \pm Z)$, it is sufficient to solve the differential equation in one octant of the cube, e.g., for $0 \leq X \leq 1$, $0 \leq Y \leq 1$, and $0 \leq Z \leq 1$. The additional boundary conditions used are

$$\begin{aligned} \frac{\partial \Phi}{\partial X}(X = 0) &= 0, & \frac{\partial \Phi}{\partial Y}(Y = 0) &= 0, & \text{and} \\ \frac{\partial \Phi}{\partial Z}(Z = 0) &= 0, \end{aligned} \quad (13)$$

which are a result of the symmetry of the potential. It should be noted that the potential is completely specified by the two parameters c_1 and r_0/ℓ_o .

A similar analysis will yield the relationship between the parameter of the Gaussian distribution of polyion charge and the experimental quantities. Subsequently, a comparison of the uniform sphere model and the Gaussian model will be made. We shall wish to relate results for the two models which correspond to equal total polyion charges whence

$$\int_V a \exp(-br^2) dV = (4/3) \pi r_o^3 A. \quad (14)$$

For the values of b of interest in this investigation, it is an excellent approximation to write

$$\int_V a \exp(-br^2) dV = 4\pi a \int_0^\infty r^2 \exp(-br^2) dr = a (\pi/b)^{3/2}. \quad (15)$$

To complete the specification of the relationship of the parameters of the two models, it is necessary to choose some criterion for the size of the polyion. It appears reasonable to require that the radius of gyration of the polyion in both models be equal, i.e.,

$$\int_V r^2 \rho_s dV = \int_V r^2 a \exp(-br^2) dV. \quad (16)$$

Evaluating the integrals with the same approximation as previously for the Gaussian model, one obtains

$$A r_o^5 = (15/8) a (\pi/b^5)^{1/2}. \quad (17)$$

Combining Eqs. (14), (15), and (17) yields

$$b = 5/(2r_o^2) \quad \text{and} \quad a = (250/9\pi)^{1/2} A = 2.9735 A. \quad (18)$$

The Poisson-Boltzmann equation for the Gaussian model may then be written as

$$\nabla^2 \Phi = 2.9735 c_1 \exp[-(5/2)(\ell_o/r_o)^2] - \exp[-\Phi]. \quad (19)$$

In order to calculate the effective diffusion constant of counterions in a polyelectrolyte solution, the following steps are necessary: (1) solution of the appropriate Poisson-Boltzmann equation for the potential in a polyelectrolyte solution, (2) solution of the differential equation for $g(x,y,z)$ using the potential obtained in the previous step, and (3) evaluation of the integrals necessary for the calculation of the diffusion ratio. We have shown how the parameters in the Poisson-Boltzmann equation are related to the experimental quantities---the per cent neutralization, degree of polymerization, and the monomer concentration. It is then possible by calculating the diffusion ratio for different values of these parameters to obtain the diffusion ratio as a function of the per cent neutralization of the polyion.

The solution of the differential equations for Φ and g and the evaluation of the integrals required for the calculation of the diffusion ratio have been carried out numerically on an IBM 7090 computer. The differential equations were solved by the method of successive block overrelaxation,^{6,7}

⁶ R. J. Arms, L. D. Gates, and B. Zondek, J. Soc. Indust. Appl. Math. 4, 220 (1956).

⁷ This method was suggested and applied to the above differential equations by R. J. Arms of the National Bureau of Standards. The Fortran program was written by P. J. Walsh of the National Bureau of Standards.

using a 20 x 20 x 20 grid of points. Iterations were continued until the maximum change in the function (g or Φ) in successive iterations was less than 10^{-4} . Usually this required about 70 iterations. The boundary conditions that the normal derivative vanish on the boundary of the cube were satisfied by requiring that the value of the function on the boundary equal its value at the neighboring interior point.

There are additional checks on the solution of the differential equations. From the boundary conditions on Φ and the divergence theorem, it is evident that $\int_V \nabla^2 \Phi \, dV = 0$. Hence, the following relationship for the volume integral of $e^{-\Phi}$ is obtained

$$\int_V e^{-\Phi} \, dV = (4\pi/3) (r_0/l_0)^3 c_1 \quad (20)$$

Since the integral of $e^{-\Phi}$ is computed numerically in the calculation of the diffusion ratio, we can compare the numerical value with that given by Eq. (20). For the 16 calculations made, the average error in the two values was 2.4% with a maximum error of 6.2%. Usually, the numerical value was smaller than the value calculated from Eq. (20).

A similar check can be used on the solution of the differential equation for g . In JC, it was shown that the average current of counterions in the x -direction is proportional to

$$I_x = \int_{-\ell_0}^{+\ell_0} \int_{-\ell_0}^{+\ell_0} e^{-\Phi} \left(1 + \frac{\partial g}{\partial x}\right) dy \, dz \quad (21)$$

and that hence in the steady state the above integral is independent of x . Since the calculation of the diffusion ratio requires the evaluation of this integral, it is possible to check the constancy of this integral for each of the twenty values of x . If, as a measure of the variation in I_x , we take the percentage difference between the maximum and minimum values of I_x , we find the average of these percentages for the 16 calculations is 3.8%. The largest percentage difference is 10.8%

The results of the numerical calculations of the effective diffusion constant are summarized in Table 1. The parameters c_1 and r_0/l_0 appearing in the table are those which occur in the Poisson-Boltzmann equation, Eq. (9) for the uniform sphere model and Eq. (19) for the Gaussian model. In Figures 1 - 16, the potential is plotted as a function of the distance R from the center of the cube along the three basic directions in the cube, viz. the x axis, the x - y diagonal, and the x - y - z diagonal. The parametric equations of the three lines are:

I	II	III	
$x = t$	$x = t$	$x = t$	
$y = 0$	$y = t$	$y = t$	
$z = 0$	$z = 0$	$z = t$	(22)

3. Discussion

It is apparent from the curves for the potential that except near the boundaries of the cube the potential is essentially a function of R alone, and not of the angular coordinates. Also for small values of R , the Donnan approximation (the assumption of zero net charge) is excellent for the potential.

For the size ratio of .684, the uniform sphere and Gaussian models can be compared. The Gaussian model gives considerably larger potential differences than the uniform sphere model. This is due to the fact that the polyion charge density at the center of the cube in the Gaussian model is approximately three times as great as in the uniform sphere model. However, even though the potential differences are larger for Gaussian model, the effective diffusion constant is usually greater for the Gaussian model, i.e., the retarding effect of the field is smaller. As the total charge is increased, the diffusion constant for the spherical model becomes smaller than its corresponding value for the Gaussian model. Even though the total change in potential is not as great for the uniform sphere model, the potential changes much more rapidly in the spherical model, i.e., the maximum electric field is greater for the uniform sphere model than for the Gaussian model.

It is interesting to note the effect on the potential of changing the polyion concentration c , leaving the other parameters, such as the per cent neutralization and the size and shape of an individual polyion, unchanged. Then from Eq. 11, as ℓ_0^3 is proportional to c^{-1} , the constant c_1 is proportional to $c^{-2/3}$. Thus going to lower values of the polyion concentration corresponds to higher values of c_1 and smaller ratios of r_0/ℓ_0 . As the effect of both of these changes is to increase the calculated potential difference, we see that one can expect higher potential differences at lower concentrations (for fixed polyion sizes). The numerical calculations S2 and S10 can be interpreted as corresponding to essentially the same values of p , s , and r_0 , with S2 corresponding to a 4.6 fold dilution from the polyion concentration of S10. The potential difference in this dilution changes from 3.45 at the higher concentration to 5.10 at the lower concentration. Wall and Berkowitz (Figure 9 of reference 4a) have also shown this increase in potential upon dilution. It seems likely that in actual polyelectrolyte solutions, the polyion will expand upon dilution and that thus the potential will not increase by such a large amount.

The diffusion constant of radioactive sodium ions in polyacrylic acid-sodium hydroxide solutions has been measured by Huizenga, Grieger, and Wall.⁵ These experiments were carried out at three different monomer concentrations and for various percentages of neutralization of the polyacrylic acid. The degree of polymerization of the polyacrylic acid was approximately one thousand (1000). In Table 2, the experimental results are summarized. Using Eq. (11) the per cent neutralization corresponding to the numerical parameters c_1 and r_0/ℓ_0 can be calculated for the three polyion concentrations. These values are given in Table 3. In Figures 17 and 18, both experimental and theoretical values of the

diffusion ratio are plotted as a function of the percentage of neutralization for the polyion concentrations of .0151 and .0378 eq./l., respectively. It is apparent from Fig. 17 that the calculations with $r_o/\ell_o = 13/19 = .684$ for the uniform sphere model fit the experimental data extremely well for all percentages of neutralization for the polyion concentration of .0151 N. For .0378 N polyacrylic acid, the theoretical points for $r_o/\ell_o = .684$ for the uniform sphere model lie slightly below the experimental results, indicating that a slightly larger value of the size ratio is required to obtain exact agreement between the experimental and theoretical diffusion ratios. Although no graph is given for .00378 N polyacrylic acid (since there is only one experimental measurement), it is evident from Tables 2 and 3 that the numerical results with $r_o/\ell_o = .684$ are again in excellent agreement with the one experimental point. Thus, it is possible with a single value of the parameter, r_o/ℓ_o , to obtain good agreement with the experimental results at three different polyion concentrations and at all percentages of neutralization.

For the Gaussian model of the charge density, a single value of the size ratio will not fit the experimental data at all percentages of neutralization. To obtain agreement with the diffusion data, it is necessary to assume that the size ratio decreases slightly as the percentage of neutralization is increased.

Before proceeding with the discussion of these results, it is desirable to point out that in the theory of the effective diffusion constant which has been presented, it has been assumed that none of the counterions are localized or site-bound to the polyion. If some of the counterions are not free, then this would change the values obtained for the effective diffusion constant in the calculation. The theory given in this report applies to the "free" counterions in the polyelectrolyte solution. Of course, the "free" counterions may be somewhat bound to the polyion by the electrostatic forces, but are not localized to a specific site on the polyion. If the fraction of free counterions is denoted by f and if the dependence of the effective diffusion constant on the percentage of neutralization is denoted by $D'(p)$, then the observed diffusion constant will be given by

$$D_{\text{obs}} = f D'(pf). \quad (23)$$

Thus, if f was known as a function of p , then the above equation could be used to obtain the observed diffusion constant as a function of the percentage of neutralization.

Assuming for the present that there are no localized ions, the numerical calculations indicate that the experimental diffusion data can be explained by taking a single size ratio, viz., $r_o/\ell_o = 0.684$. For a polymer of degree of polymerization of 1000, the monomer concentrations of .00378, .0151, and .0378 moles/liter correspond to values of ℓ_o of 380, 240, and 176 Å, respectively. The radii of the equivalent spheres needed to fit the diffusion data are then 260, 164, and 120 Å for the three concentrations. The radii of gyration of these spheres are 201, 127, and 93 Å. For a random walk model of polyacrylic acid with a statistical element

of four monomers, the radius of gyration of an uncharged polymer of degree of polymerization of 10^3 is 66 A. Experimental measurements by Oth and Doty⁸ on polymethacrylic acid indicate that this is a reasonable estimate of the size of the uncharged polymer.

The result that the size ratio necessary to fit the experimental diffusion data is essentially independent of the polymer concentration implies that the polyion size decreases as the polymer concentration increases. This conclusion is in qualitative agreement with viscosity data on polyelectrolytes. However, the result that the experimental diffusion data can be explained by a single value of the size ratio which is independent of the percentage of neutralization is in strong disagreement both with theory and with experimental measurements of the size of polyions as a function of percentage of neutralization. Since most methods of determining polymer size involve extrapolation to zero polymer concentration, no data are readily available on the size of polyions as a function of percentage neutralization at finite concentrations. However, at zero polymer concentration, the results of Oth and Doty⁸ for polymethacrylic acid indicate that the radius of the polyion changes by a factor of five or six in going from zero to one hundred per cent neutralization. Most of this change occurs at low per cent neutralization; the root mean square end to end distance increased from 210 to 940 A. from zero to 25 per cent neutralization, and at 70 per cent neutralization reached a value of 1180 A. Although the change in size is probably not as large at finite concentrations, there is undoubtedly an increase in size as the charge on the polyion is increased. The smallest percentage of neutralization for which the diffusion ratio was measured was 9.6 per cent. To explain the results obtained in the present model, it is necessary to assume that the polyion expands at low percentages of neutralization (below 9.6%), and that the size then remains fairly constant. It should also be pointed out that at low percentages of neutralization a relatively large change in the size ratio has only a small effect on the diffusion ratio.

Another possible explanation of the experimental results may be given in terms of site binding. Thus, at high per cent neutralizations, the polyion might expand to a size greater than those for which we have done our calculations leading to a higher value of the effective diffusion constant, and this increase could be compensated for by the existence of bound ions.

The authors wish to thank Dr. R. J. Arms and P. J. Walsh of the National Bureau of Standards for their assistance with the numerical computations. We also wish to thank Dr. Shneior Lifson of the Weizmann Institute of Science for his continued interest and for many helpful suggestions.

⁸ A. Oth and P. Doty, J. Phys. Chem. 56, 43 (1952).

Table 1

SUMMARY OF NUMERICAL CALCULATIONS UNIFORM SPHERE MODEL

No.	c_1	r_o/ℓ_o	D'/D
S1	100.0	.474	.72
S2	500.0	.474	.27
S3	847.0	.474	.18
S4	33.18	.684	.88
S5	99.00	.684	.64
S6	165.9	.684	.51
S7	281.0	.684	.39
S8	382.0	.684	.33
S9	108.0	.789	.66
S10	182.9	.789	.55

GAUSSIAN MODEL

No.	c_1	r_o/ℓ_o	D'/D
G1	49.17	.600	.81
G2	245.9	.600	.45
G3	416.7	.600	.36
G4	33.19	.684	.86
G5	165.9	.684	.55
G6	281.0	.684	.46

Table 2

EXPERIMENTAL DIFFUSION RATIOS*

<u>Polyion Concentration</u>	<u>Per Cent Neutralization</u>	<u>D'/D</u>
.00378 N	61.7	.63
	9.6	.92
	24.0	.79
.0151 N	41.3	.62
	61.7	.51
	81.6	.39
	97.9	.38
	9.6	.88
	24.0	.71
.0378 N	41.3	.59
	61.7	.49
	81.6	.41
	97.9	.38
	9.6	.88

* Data of Huizenga, Grieger, and Wall.

Table 3

RELATION OF NUMERICAL CALCULATIONS TO EXPERIMENT

No.	Numerical D'/D	Radius Ratio r_o / ℓ_o	Per Cent Neutralization Polyion Concentration		
			.00378 N	.0151 N	.0378 N
S1	.72	.474	18.8	11.8	.8.7
S2	.27	.474	93.8	59.1	43.5
S3	.18	.474	159.	100.	73.8
S4	.88	.684	18.7	11.8	8.7
S5	.64	.684	55.8	35.2	25.9
S6	.51	.684	93.5	58.9	43.4
S7	.39	.684	158.	99.8	73.5
S8	.33	.684	215.	136.	100.
S9	.66	.789	93.4	58.9	43.4
S10	.55	.789	158.	99.7	73.5
G1	.81	.600	18.7	11.8	8.7
G2	.45	.600	93.5	58.9	43.4
G3	.36	.600	159.	99.9	73.6
G4	.86	.684	18.7	11.8	8.7
G5	.55	.684	93.5	58.9	43.4
G6	.46	.684	158.	99.8	73.5

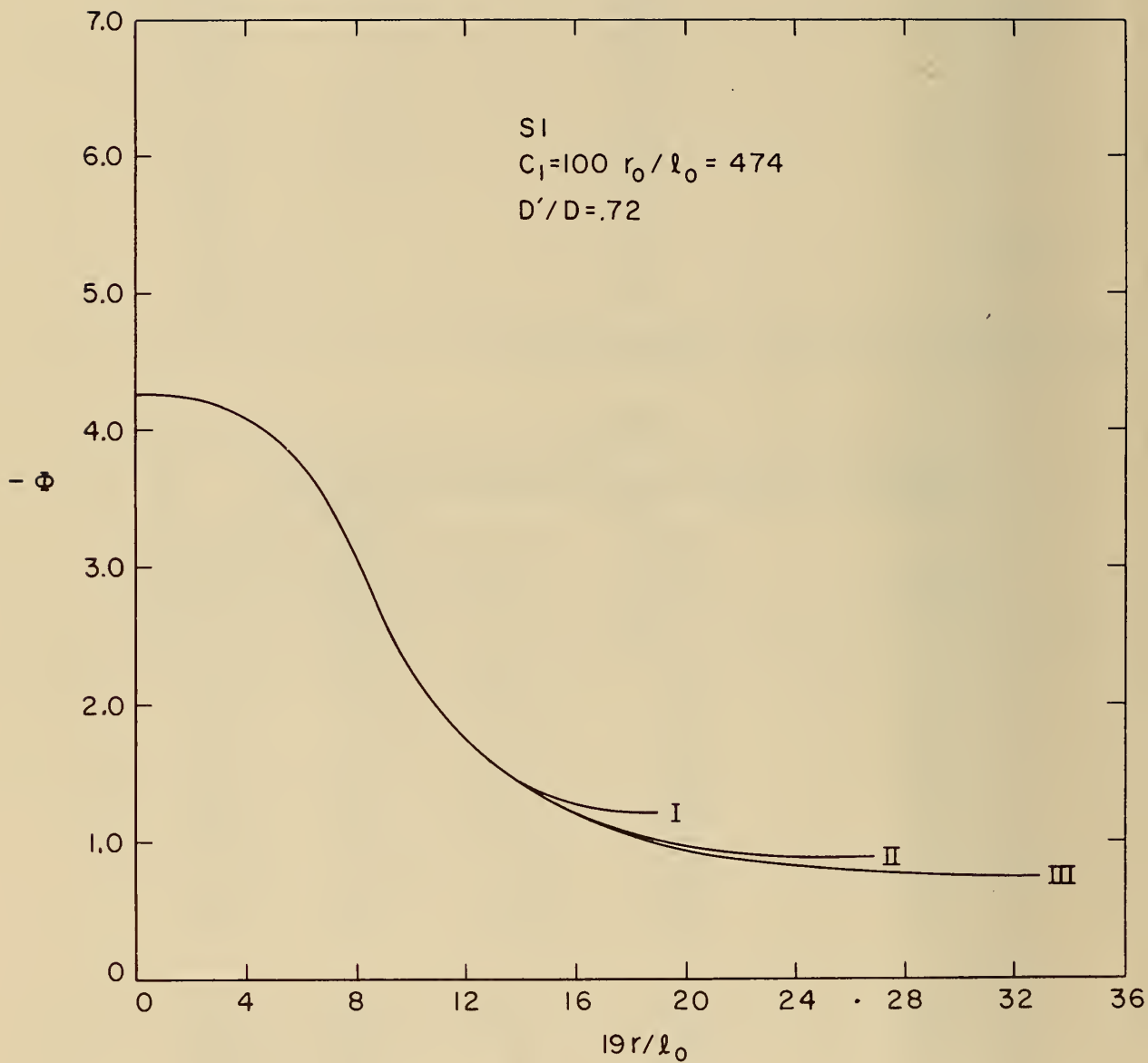


Figure 1. The potential as a function of relative distance from the center of the polyion.

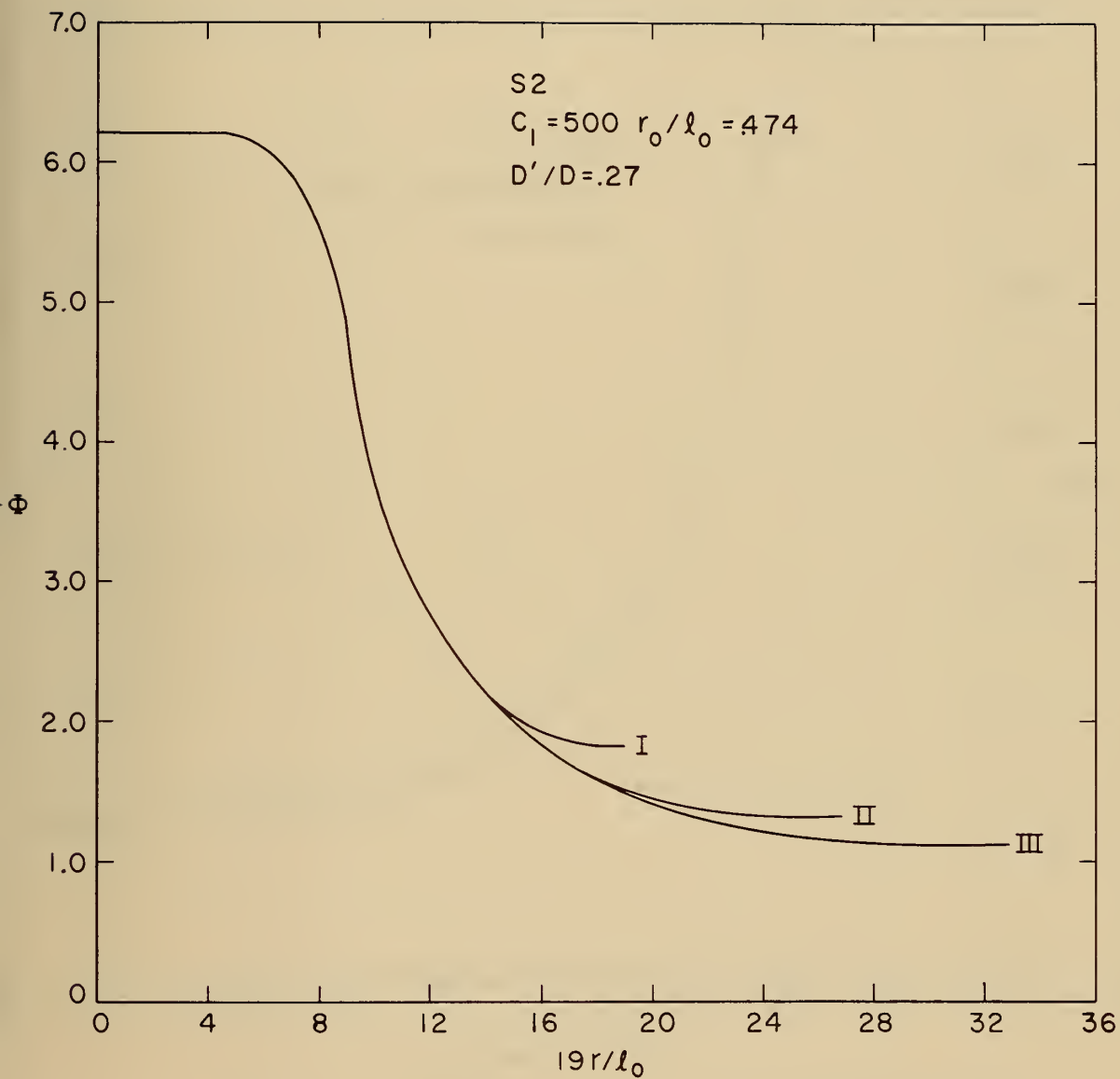


Figure 2. The potential as a function of relative distance from the center of the polyion.

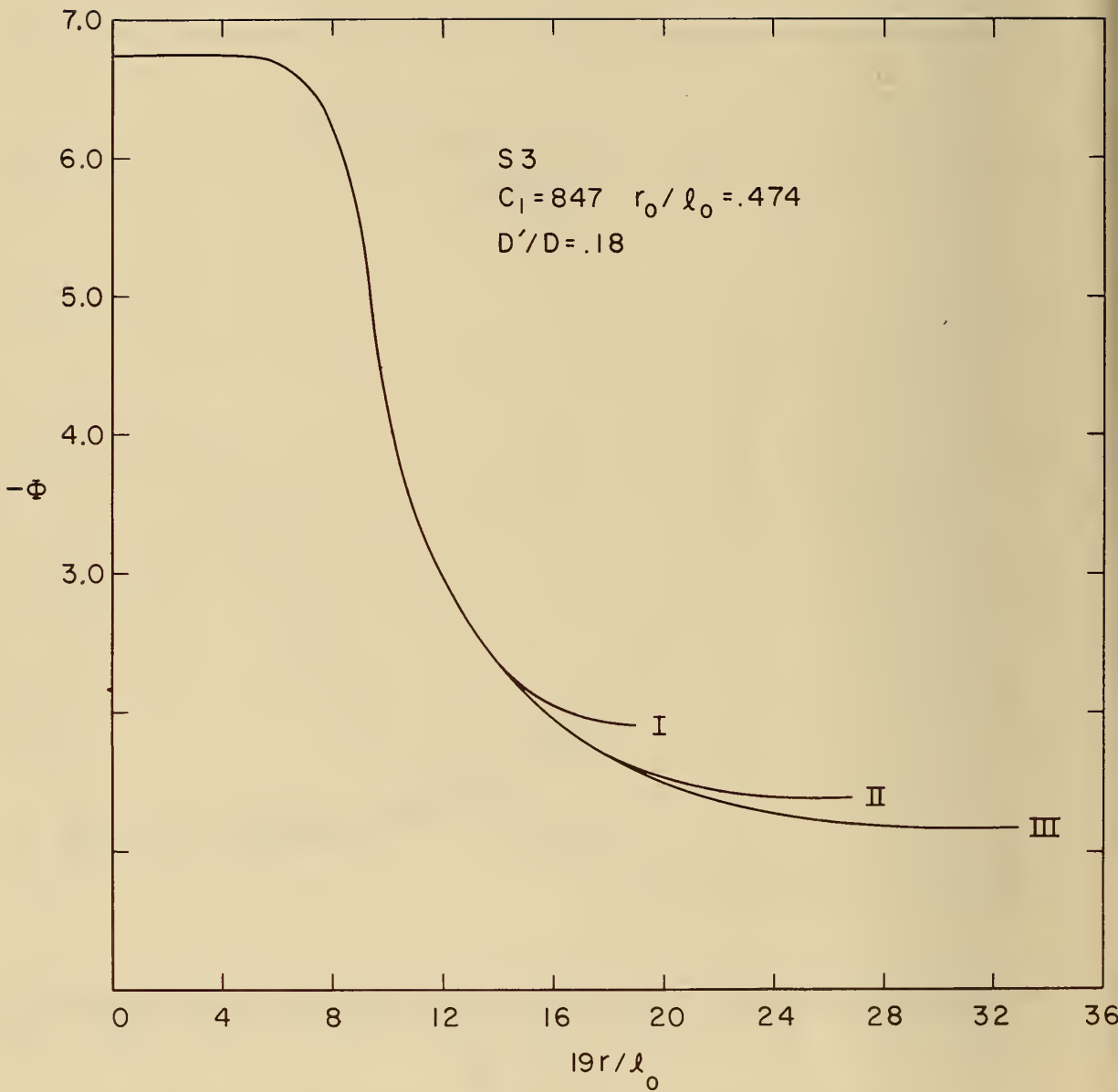


Figure 3. The potential as a function of relative distance from the center of the polyion.

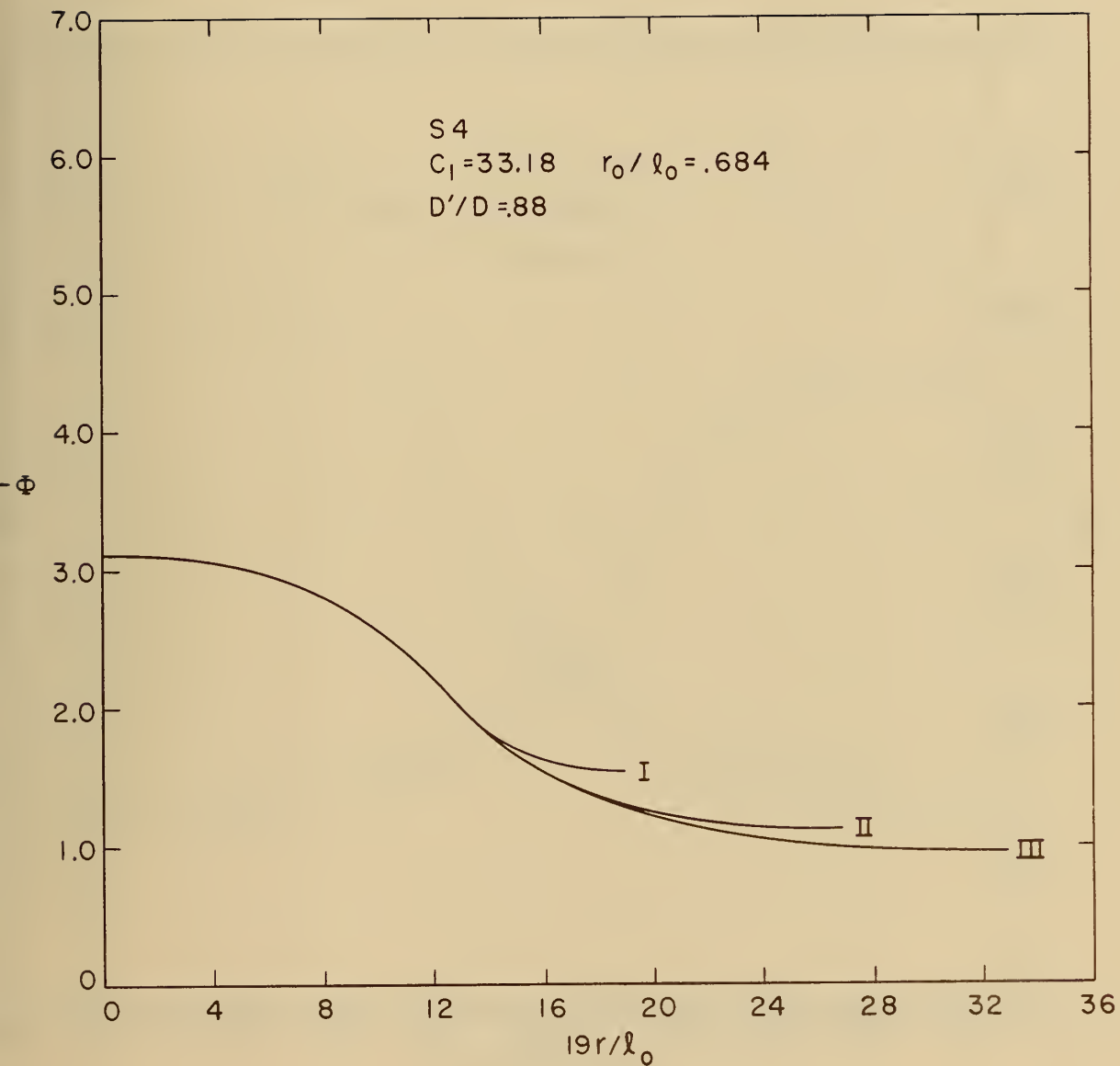


Figure 4. The potential as a function of relative distance from the center of the polyion.

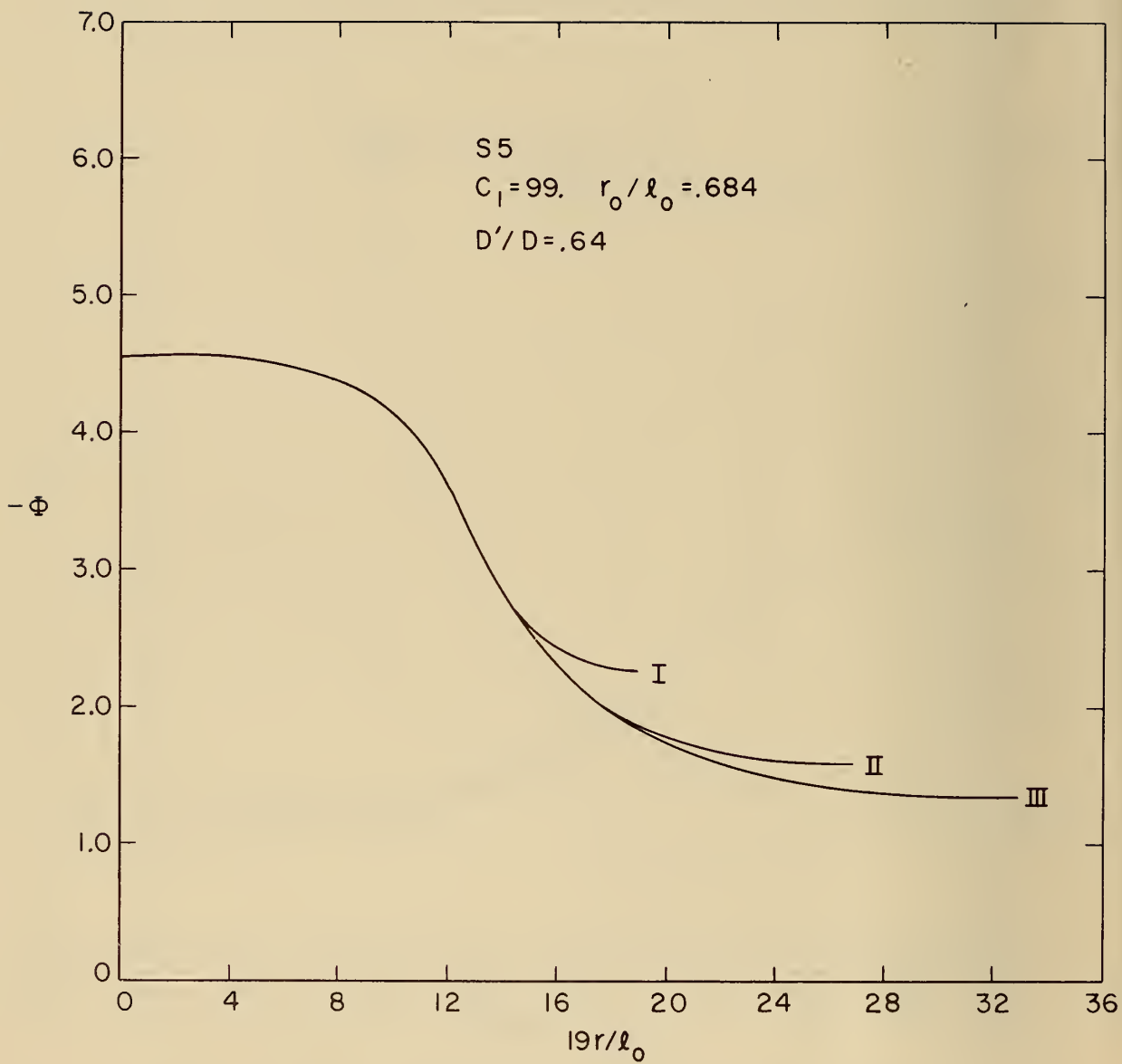


Figure 5. The potential as a function of relative distance from the center of the polyion.

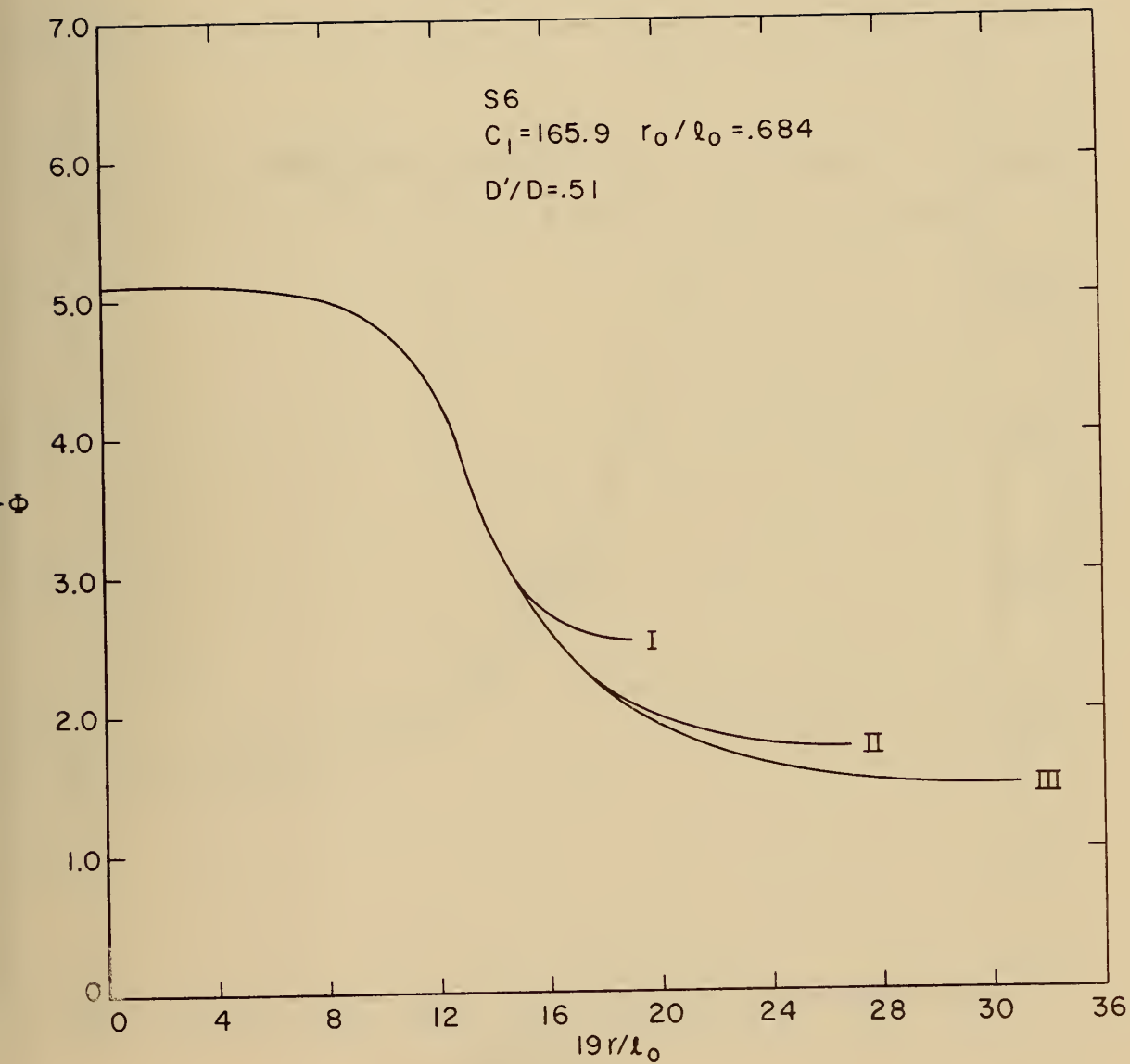


Figure 6. The potential as a function of relative distance from the center of the polyion.

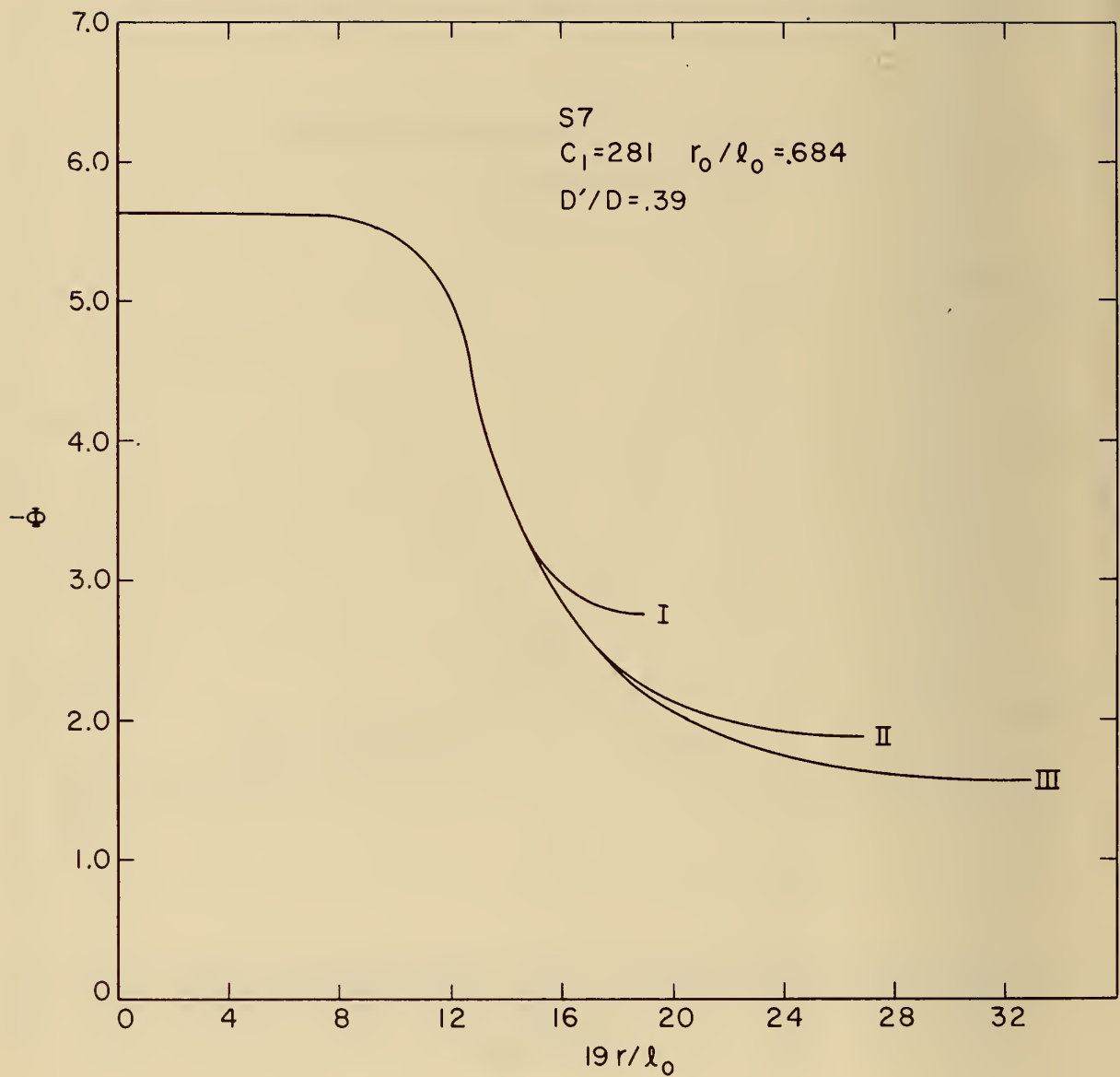


Figure 7. The potential as a function of relative distance from the center of the polyion.

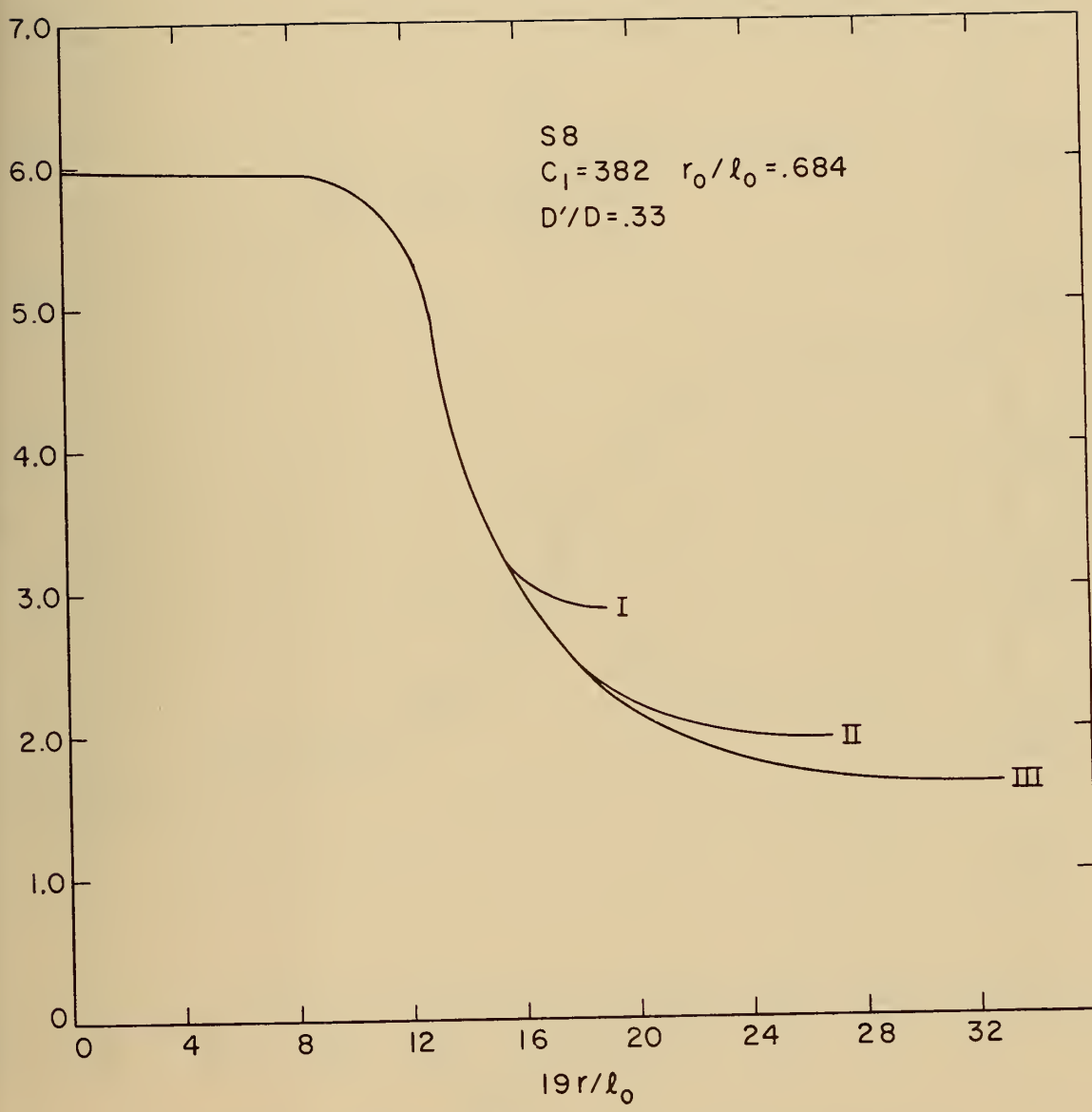


Figure 8. The potential as a function of relative distance from the center of the polyion.

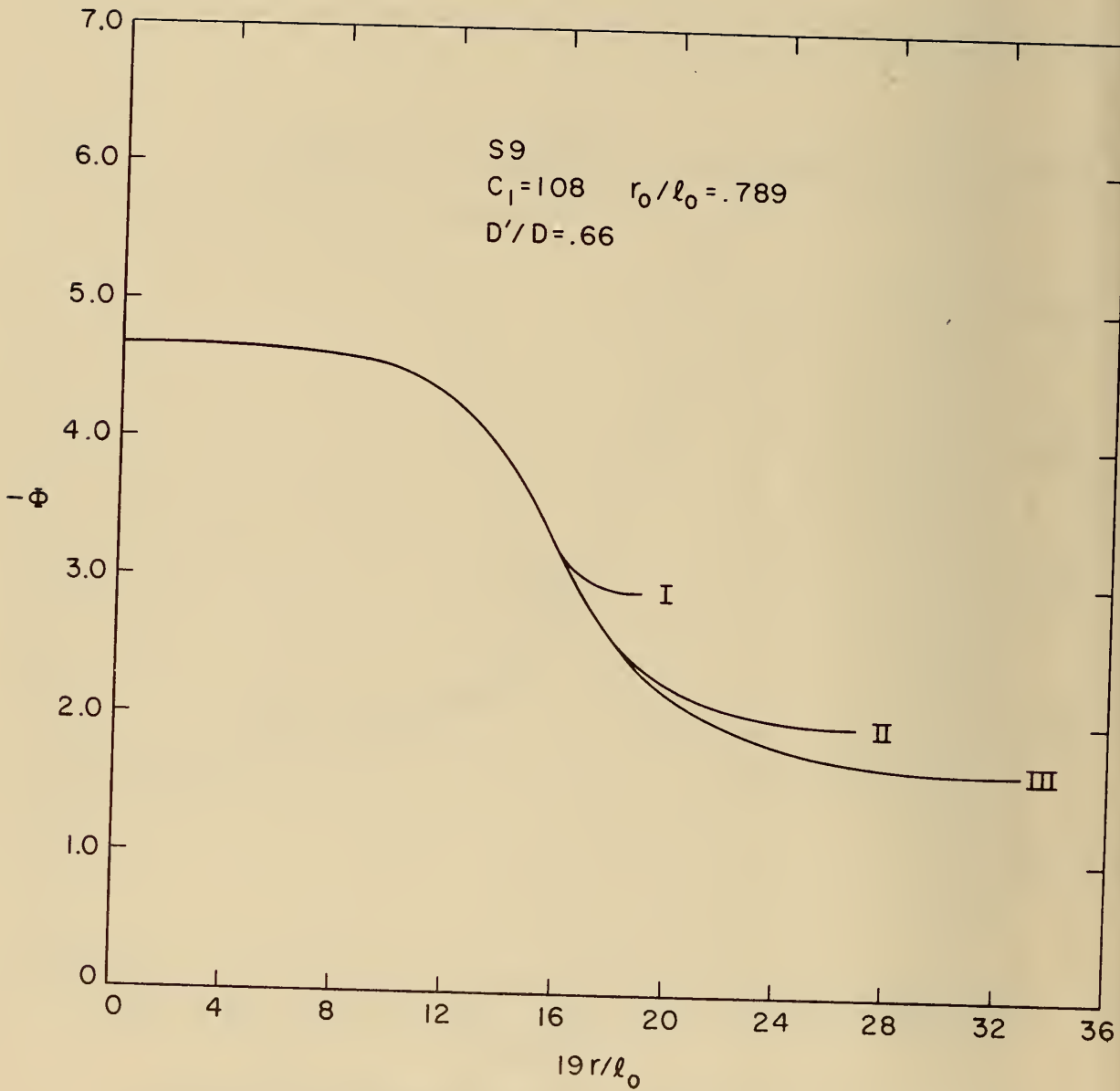


Figure 9. The potential as a function of relative distance from the center of the polyion.

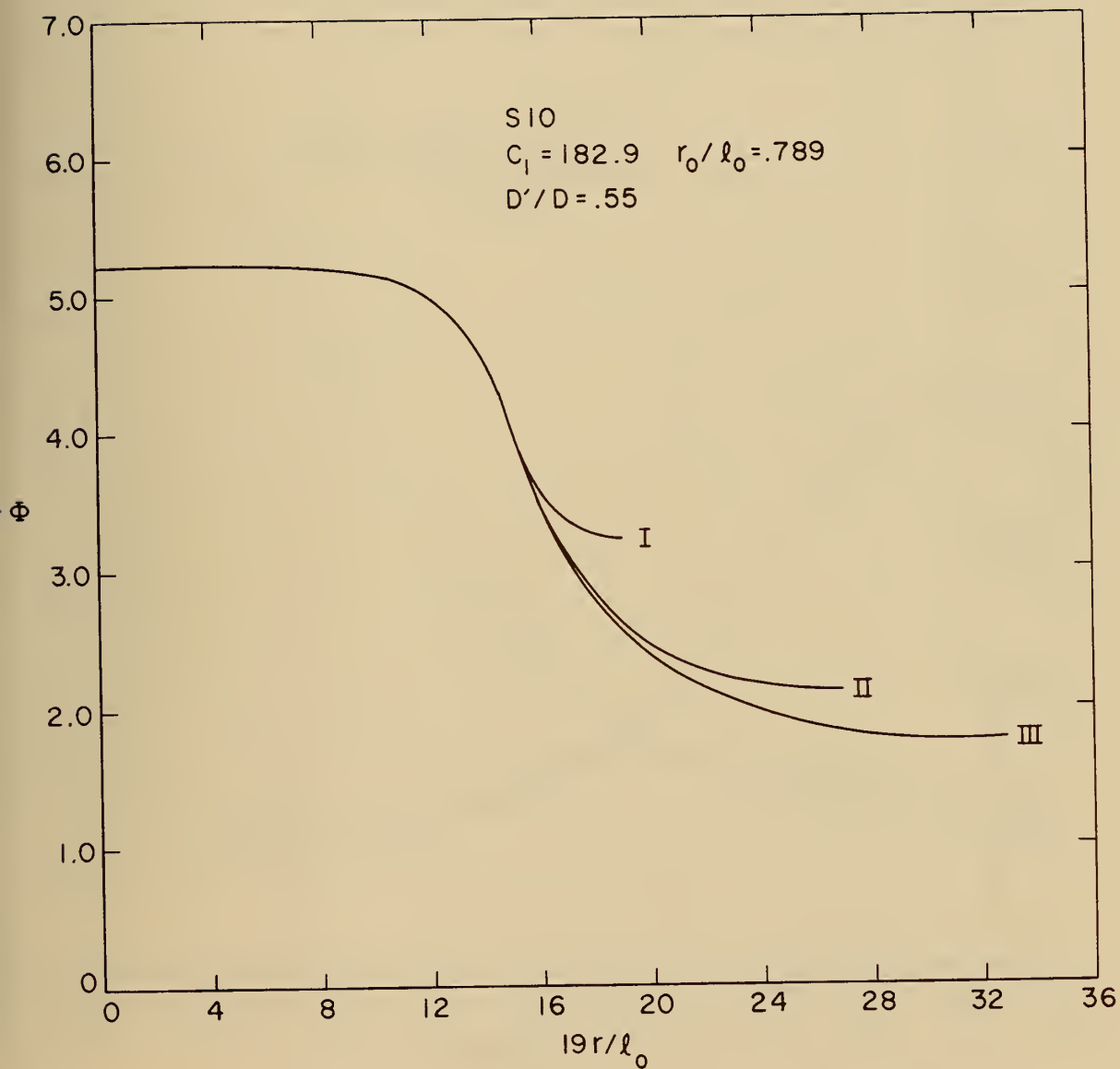


Figure 10. The potential as a function of relative distance from the center of the polyion.

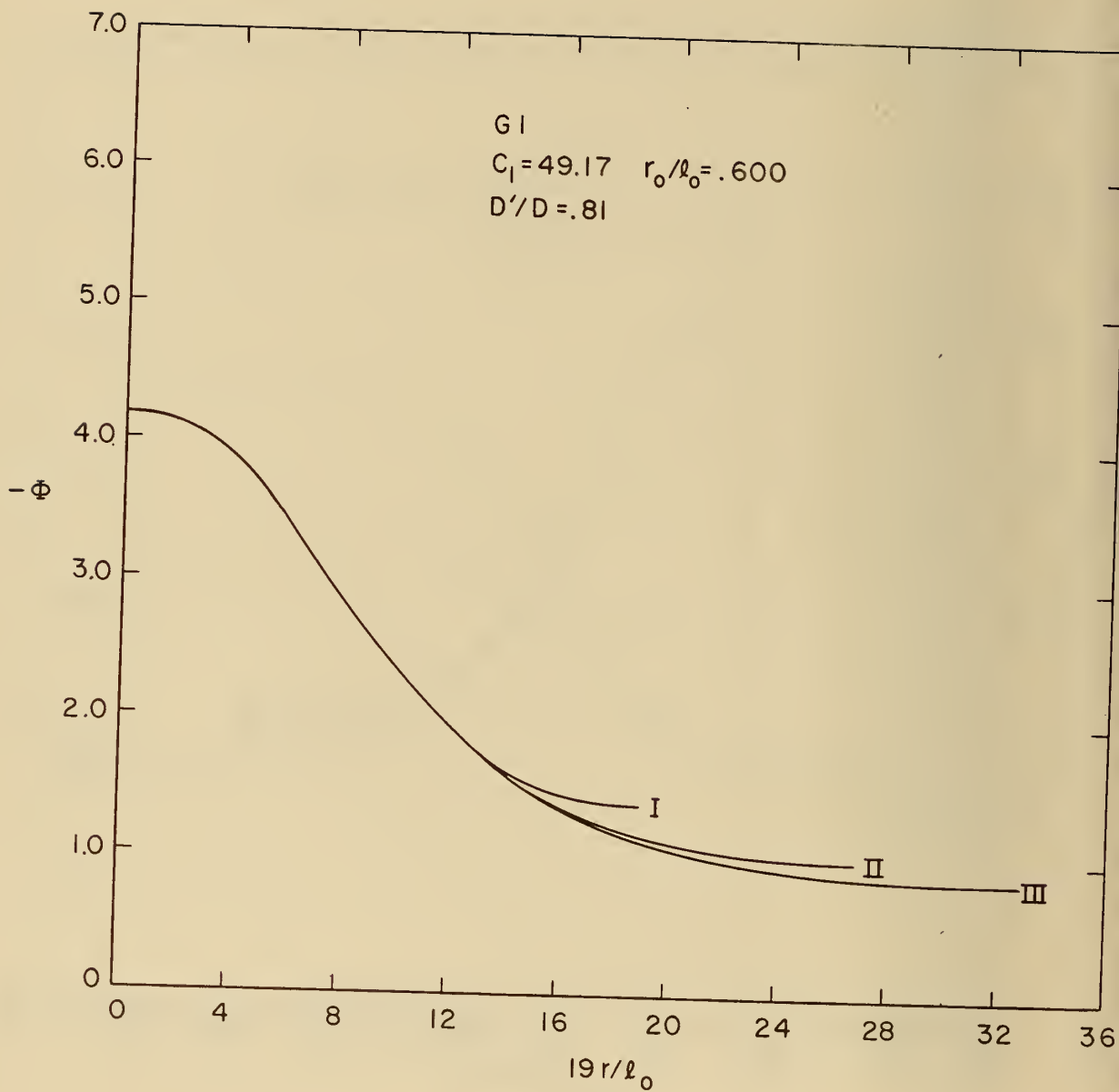


Figure 11. The potential as a function of relative distance from the center of the polyion.

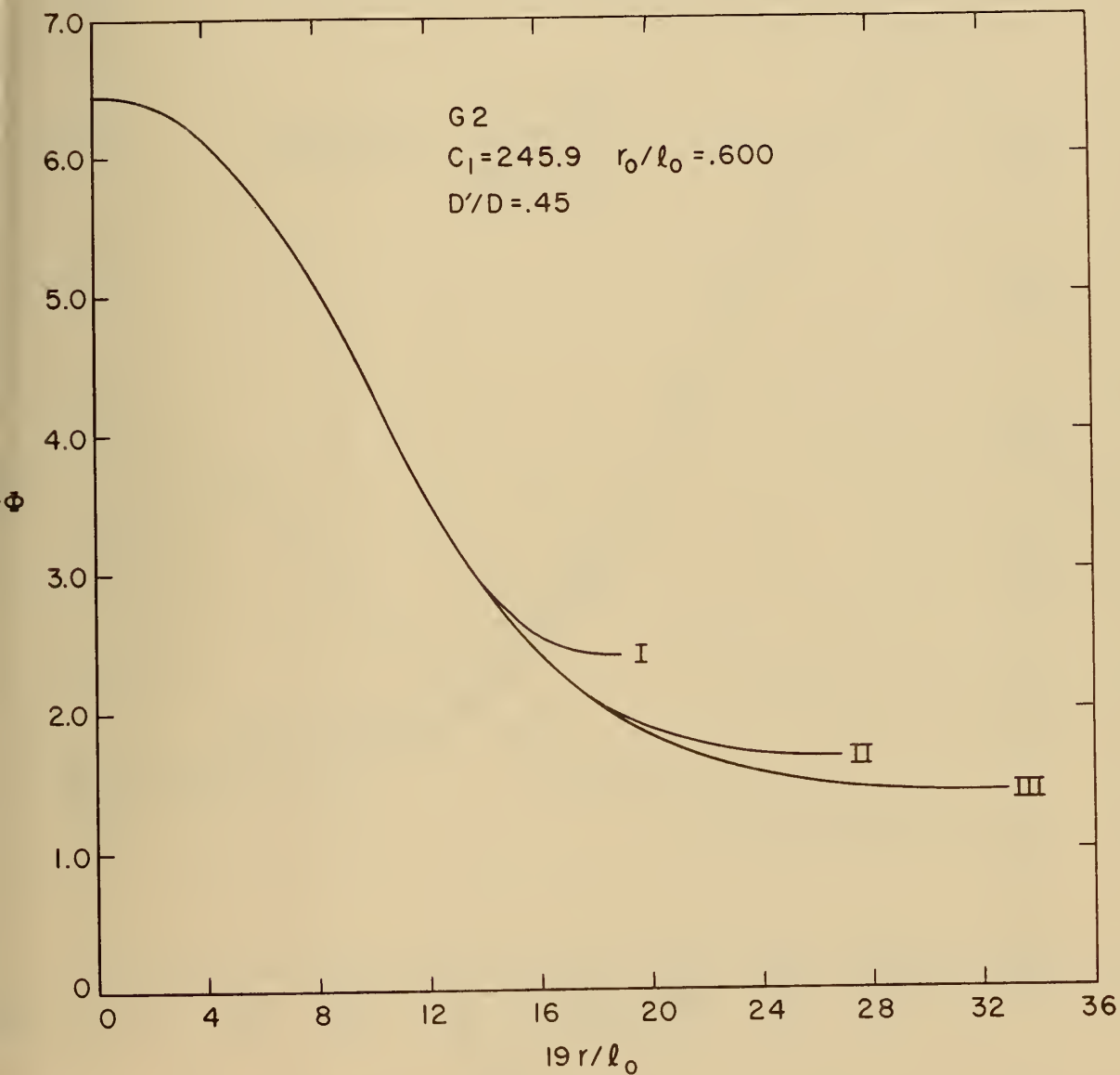


Figure 12. The potential as a function of relative distance from the center of the polyion.

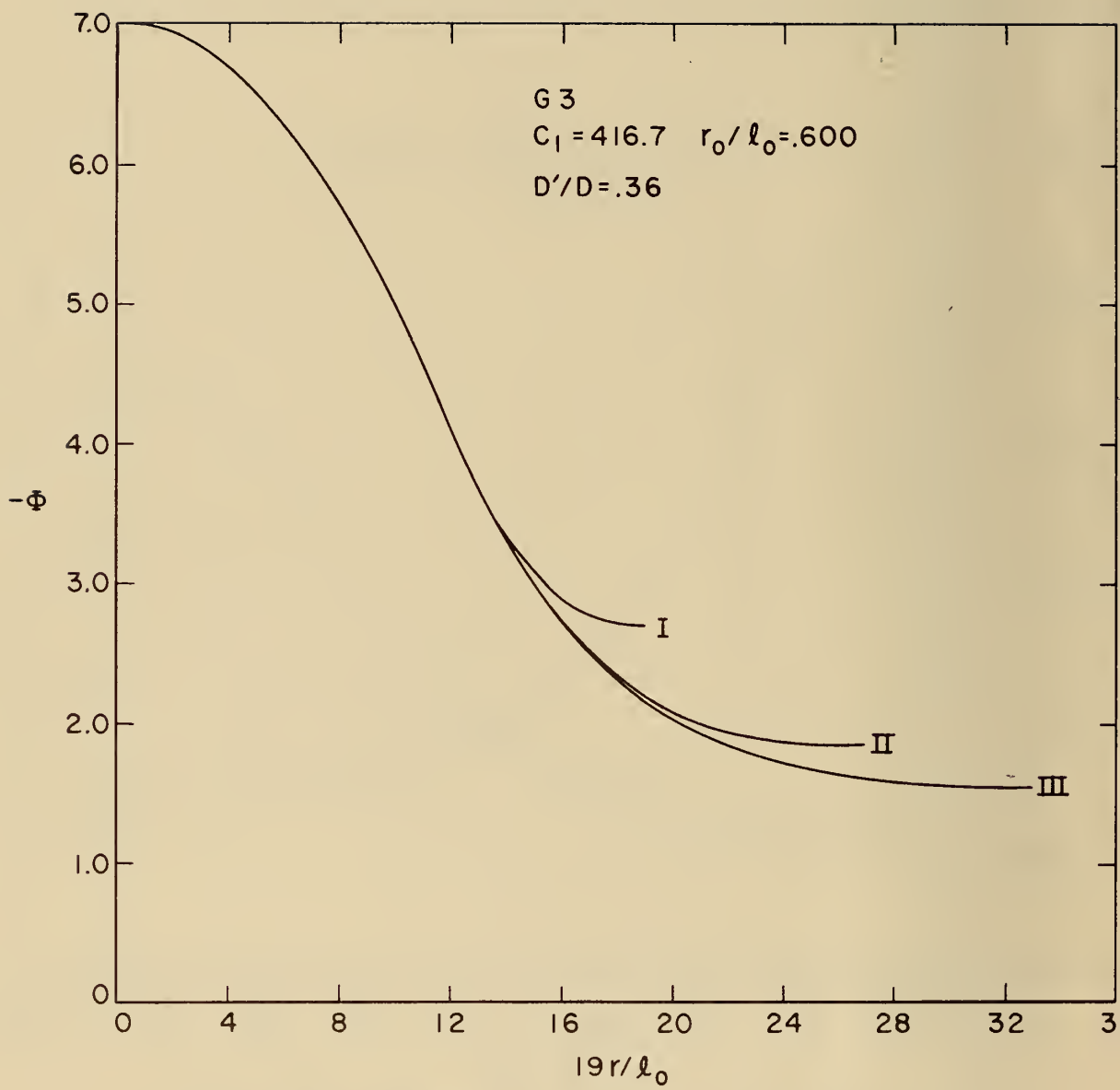


Figure 13. The potential as a function of relative distance from the center of the polyion.

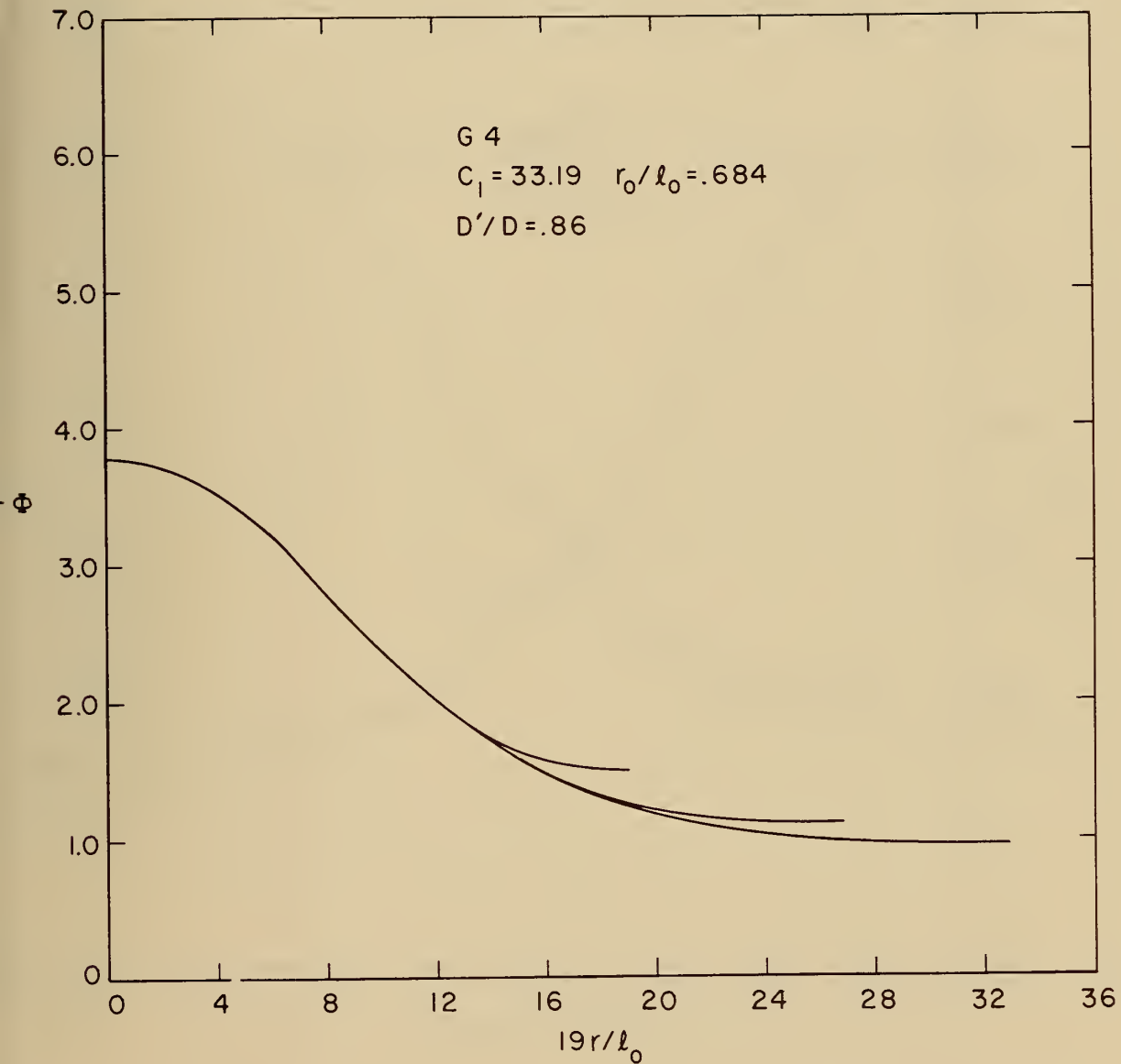


Figure 14. The potential as a function of relative distance from the center of the polyion.

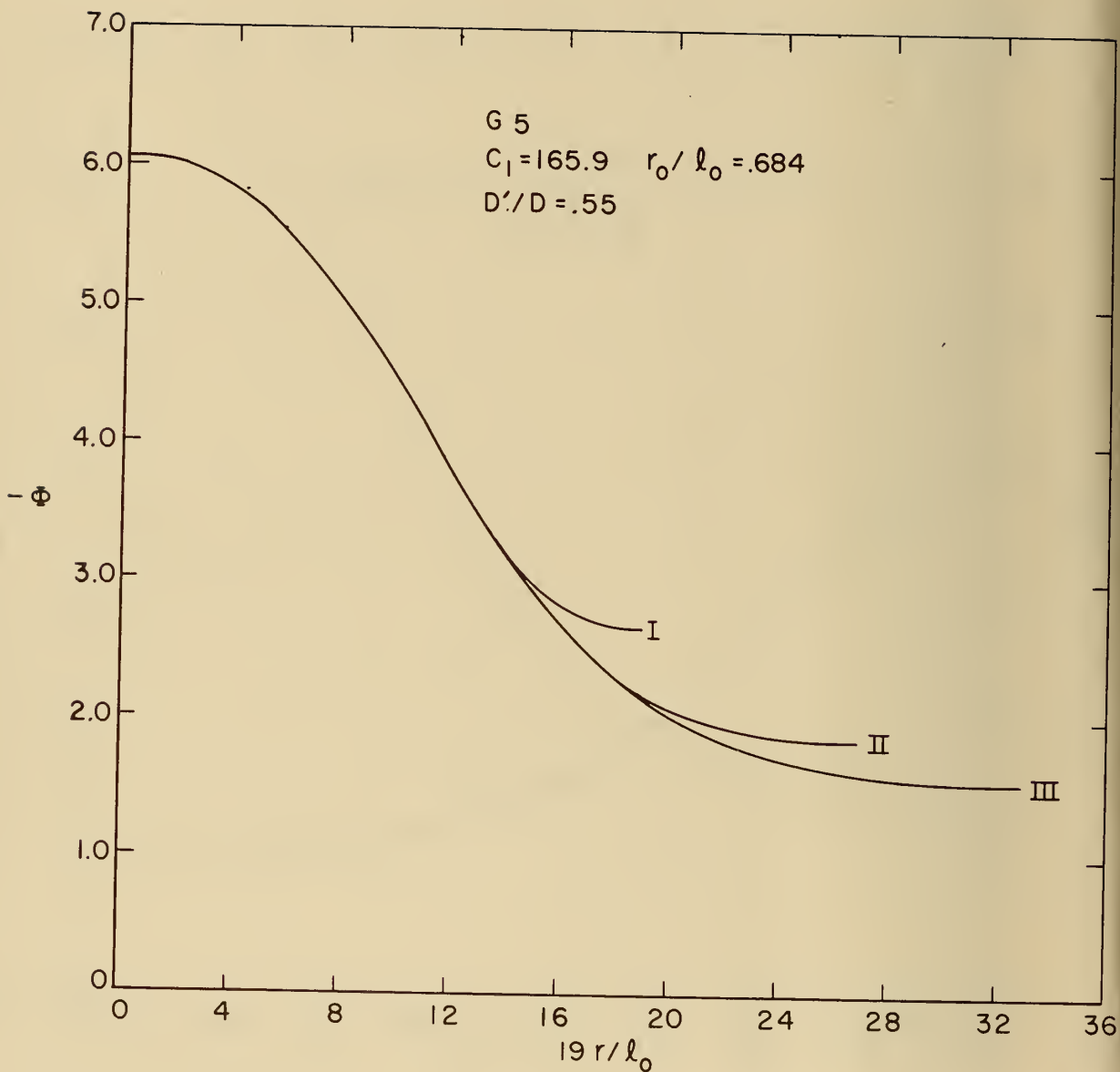


Figure 15. The potential as a function of relative distance from the center of the polyion.

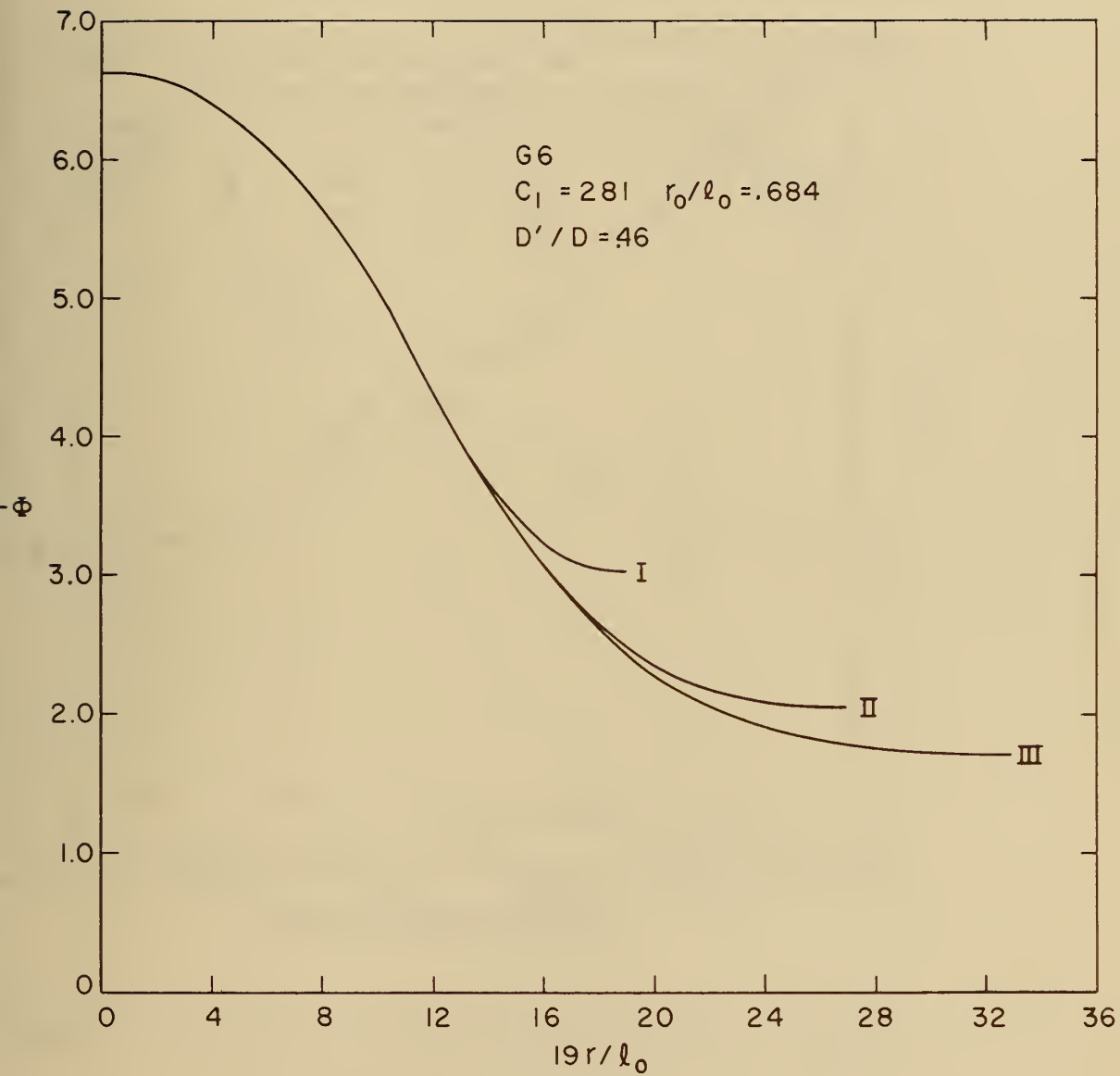


Figure 16. The potential as a function of relative distance from the center of the polyion.

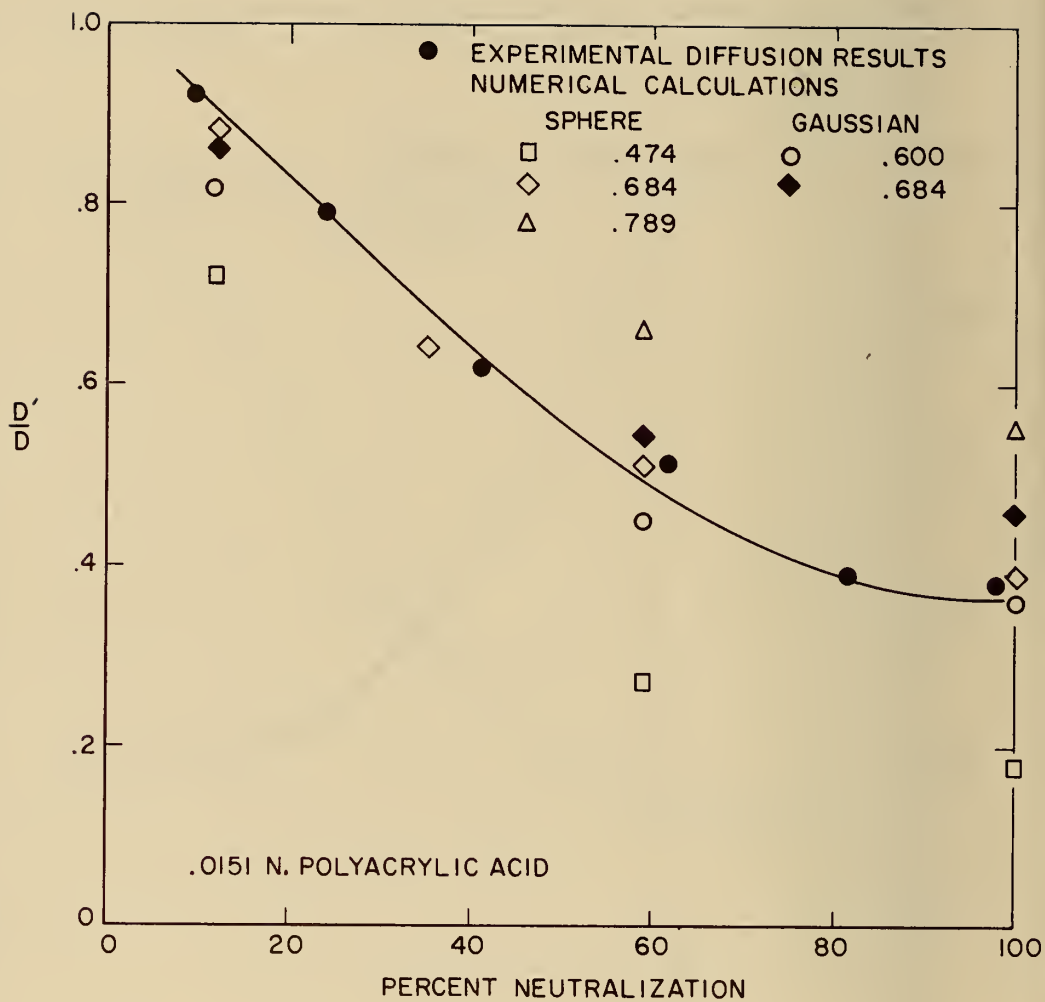


Figure 17. The diffusion ratio D'/D as a function of per cent neutralization.

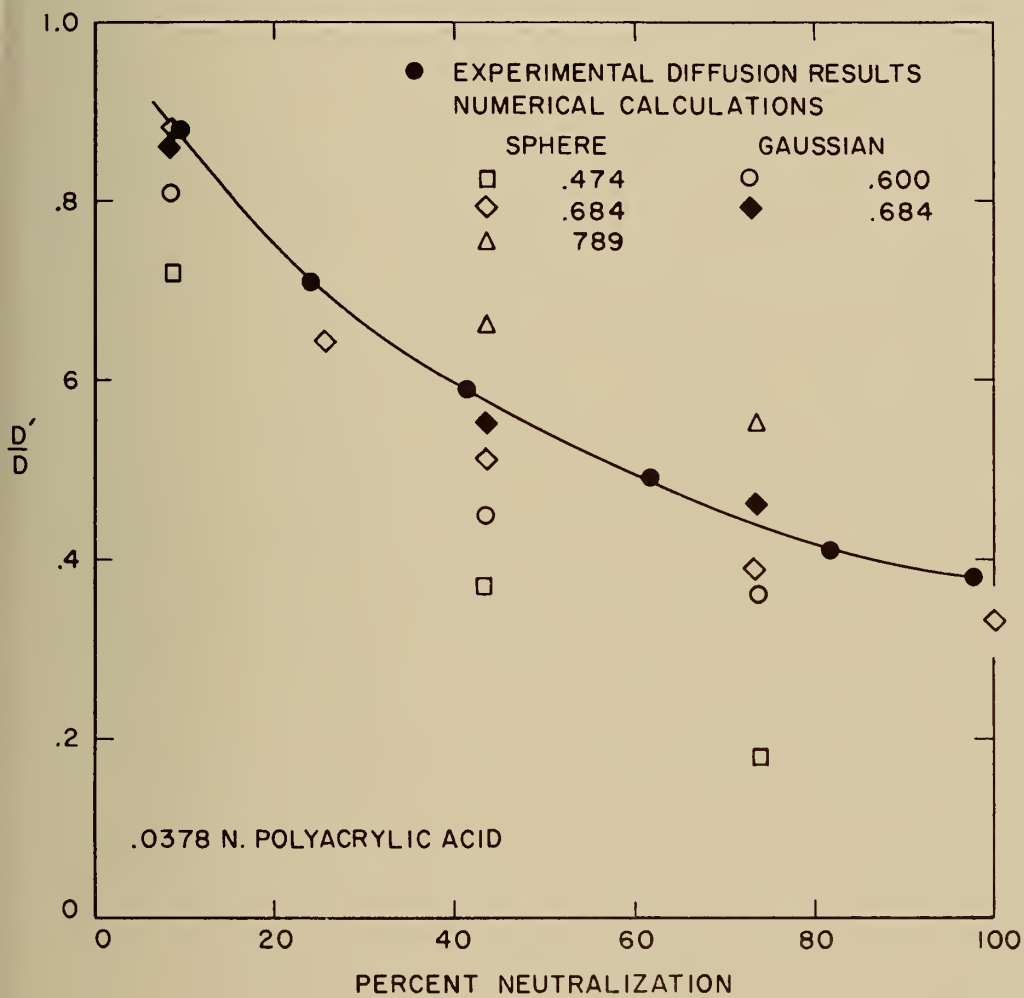


Figure 18. The diffusion ratio D'/D as a function of per cent neutralization.



THE NATIONAL BUREAU OF STANDARDS

The scope of activities of the National Bureau of Standards at its major laboratories in Washington, D.C., and Boulder, Colorado, is suggested in the following listing of the divisions and sections engaged in technical work. In general, each section carries out specialized research, development, and engineering in the field indicated by its title. A brief description of the activities, and of the resultant publications, appears on the inside of the front cover.

WASHINGTON, D. C.

Electricity. Resistance and Reactance. Electrochemistry. Electrical Instruments. Magnetic Measurements. Dielectrics. High Voltage. Absolute Electrical Measurements.

Metrology. Photometry and Colorimetry. Refractometry. Photographic Research. Length. Engineering Metrology. Mass and Volume.

Heat. Temperature Physics. Heat Measurements. Cryogenic Physics. Equation of State. Statistical Physics.

Radiation Physics. X-ray. Radioactivity. Radiation Theory. High Energy Radiation. Radiological Equipment. Nucleonic Instrumentation. Neutron Physics.

Analytical and Inorganic Chemistry. Pure Substances. Spectrochemistry. Solution Chemistry. Standard Reference Materials. Applied Analytical Research. Crystal Chemistry.

Mechanics. Sound. Pressure and Vacuum. Fluid Mechanics. Engineering Mechanics. Rheology. Combustion Controls.

Polymers. Macromolecules: Synthesis and Structure. Polymer Chemistry. Polymer Physics. Polymer Characterization. Polymer Evaluation and Testing. Applied Polymer Standards and Research. Dental Research.

Metallurgy. Engineering Metallurgy. Metal Reactions. Metal Physics. Electrolysis and Metal Deposition.

Inorganic Solids. Engineering Ceramics. Glass. Solid State Chemistry. Crystal Growth. Physical Properties. Crystallography.

Building Research. Structural Engineering. Fire Research. Mechanical Systems. Organic Building Materials. Codes and Safety Standards. Heat Transfer. Inorganic Building Materials. Metallic Building Materials.

Applied Mathematics. Numerical Analysis. Computation. Statistical Engineering. Mathematical Physics. Operations Research.

Data Processing Systems. Components and Techniques. Computer Technology. Measurements Automation. Engineering Applications. Systems Analysis.

Atomic Physics. Spectroscopy. Infrared Spectroscopy. Far Ultraviolet Physics. Solid State Physics. Electron Physics. Atomic Physics. Plasma Spectroscopy.

Instrumentation. Engineering Electronics. Electron Devices. Electronic Instrumentation. Mechanical Instruments. Basic Instrumentation.

Physical Chemistry. Thermochemistry. Surface Chemistry. Organic Chemistry. Molecular Spectroscopy. Elementary Processes. Mass Spectrometry. Photochemistry and Radiation Chemistry.

Office of Weights and Measures.

BOULDER, COLO.

CRYOGENIC ENGINEERING LABORATORY

Cryogenic Processes. Cryogenic Properties of Solids. Cryogenic Technical Services. Properties of Cryogenic Fluids.

CENTRAL RADIO PROPAGATION LABORATORY

Ionosphere Research and Propagation. Low Frequency and Very Low Frequency Research. Ionosphere Research. Prediction Services. Sun-Earth Relationships. Field Engineering. Radio Warning Services. Vertical Soundings Research.

Troposphere and Space Telecommunications. Data Reduction Instrumentation. Radio Noise. Tropospheric Measurements. Tropospheric Analysis. Spectrum Utilization Research. Radio-Meteorology. Lower Atmosphere Physics.

Radio Systems. Applied Electromagnetic Theory. High Frequency and Very High Frequency Research. Frequency Utilization. Modulation Research. Antenna Research. Radiodetermination.

Upper Atmosphere and Space Physics. Upper Atmosphere and Plasma Physics. High Latitude Ionosphere Physics. Ionosphere and Exosphere Scatter. Airglow and Aurora. Ionospheric Radio Astronomy.

RADIO STANDARDS LABORATORY

Radio Standards Physics. Frequency and Time Disseminations. Radio and Microwave Materials. Atomic Frequency and Time-Interval Standards. Radio Plasma. Microwave Physics.

Radio Standards Engineering. High Frequency Electrical Standards. High Frequency Calibration Services. High Frequency Impedance Standards. Microwave Calibration Services. Microwave Circuit Standards. Low Frequency Calibration Services.

Joint Institute for Laboratory Astrophysics-NBS Group (Univ. of Colo.).

